



Cite this: DOI: 10.1039/c7nj03728g

# One-step selective synthesis of 2-chlorobenzonitrile from 2-chlorotoluene via ammoxidation†

Hari Babu B., \*<sup>abc</sup> Venkateswara Rao K. T.,<sup>a</sup> Suh Y. W., <sup>bc</sup> Sai Prasad P. S. \*<sup>a</sup> and Lingaiah N.\*<sup>a</sup>

A series of V<sub>2</sub>O<sub>5</sub>/Al<sub>2</sub>O<sub>3</sub> catalysts were prepared by a wet impregnation method and employed for a one-step synthesis of 2-chlorobenzonitrile from 2-chlorotoluene via ammoxidation in a fixed bed reactor at atmospheric pressure. The catalysts were characterized by BET-SA, XRD, FT-IR, TPR, UV-Vis DRS and NH<sub>3</sub>-TPD to identify the molecular structural changes of the catalysts. The characterization results revealed that the addition of V<sub>2</sub>O<sub>5</sub> to Al<sub>2</sub>O<sub>3</sub> amplified the crystallinity of alumina and also resulted in the formation of an interactive species *i.e.* AlVO<sub>4</sub>. Most of the V<sub>2</sub>O<sub>5</sub> existed in the form of isolated surface and polymeric tetrahedral vanadia species in a highly dispersed state and/or having a strong interaction with the support. The formation of different kinds of vanadia species was entirely dependent on the content of vanadia present in the catalyst. A 10 wt% V<sub>2</sub>O<sub>5</sub>/Al<sub>2</sub>O<sub>3</sub> catalyst was found to be the best and the high selectivity for 2-CBN was presumably due to the formation of the isolated surface and polymeric tetrahedral vanadia species along with aluminum vanadate species.

Received 29th September 2017,  
Accepted 13th December 2017

DOI: 10.1039/c7nj03728g

rsc.li/njc

## 1. Introduction

Vanadium oxide has extensive applications in industrially important reactions. However, it cannot be used in its bulk form because of its poor thermal stability and mechanical strength. In addition, it causes fast catalyst deactivation and favors deep oxidation. For this reason, V<sub>2</sub>O<sub>5</sub> is usually supported on inorganic oxides such as TiO<sub>2</sub>, ZrO<sub>2</sub>, SiO<sub>2</sub> and γ-Al<sub>2</sub>O<sub>3</sub>. Generally, a support offers a sufficient surface area for a metal or metal oxide dispersion and enhances the number of active sites and also improves the mechanical strength and thermal stability. The surface structure of supported vanadia species is different from that of the bulk phase and consequently plays a unique role in catalytic performance. Supported vanadia catalysts are well-known and extensively employed in a variety of industrial processes such as oxidation of hydrocarbons,<sup>1</sup> methanol oxidation,<sup>2</sup> oxidative dehydrogenation of alkanes,<sup>3</sup> selective catalytic reduction of NO<sub>x</sub> with NH<sub>3</sub>,<sup>4</sup> and ammoxidation of substituted aromatic and heteroaromatic compounds.<sup>5,6</sup>

Supports play a vital role in influencing vanadia dispersions and thereby the activity and selectivity of vanadia catalysts. Lemonidou *et al.*<sup>7</sup> studied the oxidative dehydrogenation (ODH) of propane over various supported vanadia catalysts and concluded that V<sub>2</sub>O<sub>5</sub>/TiO<sub>2</sub> is the most active catalyst whereas V<sub>2</sub>O<sub>5</sub>/Al<sub>2</sub>O<sub>3</sub> is the most selective catalyst. It is well-known that γ-Al<sub>2</sub>O<sub>3</sub> allows the dispersion of vanadium cations by facilitating the formation of inter-connected tetrahedral vanadate VO<sub>4</sub><sup>3-</sup> units sharing corners and forming a two dimensional layer.<sup>8,9</sup> Eon *et al.*<sup>10</sup> studied the ODH of propane with V<sub>2</sub>O<sub>5</sub>/Al<sub>2</sub>O<sub>3</sub> catalysts and found that the bridging V–O–V groups from a two-dimensional VO<sub>4</sub> arrangement are the active sites for this reaction. Supports are often found to modify the physico-chemical properties of vanadia catalysts. Traditionally, vanadia catalysts supported on Al<sub>2</sub>O<sub>3</sub> and ZrO<sub>2</sub> are found to be active for the ammoxidation of toluene.<sup>11,12</sup> Likewise, Reddy *et al.*<sup>13,14</sup> studied the ammoxidation of 3-picoline over V<sub>2</sub>O<sub>5</sub>/Al<sub>2</sub>O<sub>3</sub> catalysts. Even though Al<sub>2</sub>O<sub>3</sub> supported V<sub>2</sub>O<sub>5</sub> catalysts are studied for ammoxidation reactions, there has been a lot of scope to apply these materials to other methyl aromatics.

Conversely, halogen substituted benzonitriles have a wide range of applications in the fine chemical industry for the synthesis of different dyestuffs, herbicides, pharmaceuticals, and pesticides.<sup>15–19</sup> Hence, the preparation of these compounds by ammoxidation is of particular interest. In particular, 2-chlorobenzonitrile is an important chemical intermediate used for the production of industrially important azo dyes namely,

<sup>a</sup> Catalysis Laboratory, I&PC Division, CSIR-Indian Institute of Chemical Technology, Hyderabad 500 007, India. E-mail: haribabu.bathula@gmail.com

<sup>b</sup> Department of Chemical Engineering, Hanyang University, Seoul 133-691, Republic of Korea

<sup>c</sup> Research Institute of Industrial Science, Hanyang University, Seoul 133-691, Republic of Korea

† Electronic supplementary information (ESI) available. See DOI: 10.1039/c7nj03728g

2-amino-5-nitrobenzotrile and 2-cyano-4-nitroaniline. Another dynamic use of 2-chlorobenzotrile is its utilization as a starting material for the synthesis of 2-chlorobenzylamine, which can be used as an analgesic, antihypertensive, antitumor active, blood stream disorder disease remedy, anticoagulant, antifolate and anticholesteremic agent.<sup>20</sup> From a bibliographic standpoint, only few have reported the synthesis of 2-chlorobenzotrile (2-CBN) from 2-chlorotoluene (2-CT) by means of an ammoxidation process. Comparatively, inadequate literature is available on the ammoxidation of 2-chlorotoluene over other alkyl aromatics. Ammonium containing vanadium phosphate,<sup>21–23</sup> alumina supported  $V_2O_5$ <sup>19</sup> and DC-108 (composition not disclosed)<sup>24</sup> catalysts were effective for this reaction. The formation of undesirable by-products led to low selectivity towards the nitrile compound over these catalysts. Therefore, it is highly desirable to develop a heterogeneous catalyst for ammoxidation of 2-chlorotoluene which would yield high selectivity towards 2-CBN.

Recently, we demonstrated the influence of various promoters (*i.e.*  $MoO_3$ ,  $WO_3$  and  $La_2O_3$ ) and their loading on the structural and catalytic functionalities of  $V_2O_5/Al_2O_3$  catalysts for ammoxidation of 2-chlorotoluene.<sup>18</sup> All those catalysts selectively yielded 2-chlorobenzotrile from 2-chlorotoluene *via* ammoxidation. The present investigation depicts the effect of  $V_2O_5$  loading and reaction temperature on the catalytic performance of  $V_2O_5/Al_2O_3$  catalysts in the ammoxidation of 2-chlorotoluene and also finding the reason for selective formation of 2-chlorobenzotrile is one more objective of this study. The catalysts prepared with different  $V_2O_5$  loadings have been characterized by various physico-chemical techniques to identify the active species responsible for the ammoxidation activity. Correlations have been drawn between the physico-chemical properties of the catalysts and the activity and selectivity in the ammoxidation of 2-chlorotoluene to 2-chlorobenzotrile.

## 2. Experimental

### 2.1. Preparation of the catalysts

All the chemicals employed were of analytical grade and used as received without further purification. Ammonium metavanadate ( $NH_4VO_3$ ) and oxalic acid ( $C_2H_2O_4$ ) were purchased from S.D. Fine Chem. Pvt. Ltd, India, whereas the support,  $\gamma-Al_2O_3$ , was supplied by Engelhard. A series of alumina supported  $V_2O_5$  catalysts were prepared by varying the vanadium content from 5 to 15 wt%, by a conventional wet impregnation method. In this method, impregnation of the  $Al_2O_3$  support was carried out with a solution of a vanadium oxalate precursor. To prepare 5 wt%  $V_2O_5/Al_2O_3$  catalyst, the vanadium oxalate precursor solution was prepared by adding 0.68 g of ammonium metavanadate to 1.05 g of oxalic acid in a molar ratio of 1:2. The resulting mixture was thoroughly stirred at room temperature until complete dissolution of the solid. The color of the solution turned deep blue. After that, this solution was added to 10 g of  $\gamma-Al_2O_3$  support under constant stirring. The excess water was removed using a water bath and the catalyst masses were dried in an air oven at 120 °C for 12 h. Finally, the catalyst

was obtained by calcination at 450 °C for 4 h in an air flow. The same procedure was used for the preparation of 10 and 15 wt%  $V_2O_5/Al_2O_3$  catalysts by varying the amounts of ammonium metavanadate and oxalic acid. This series of catalysts were denoted by their weight percentage of  $V_2O_5$ . For example 5 wt%  $V_2O_5/Al_2O_3$  indicates that the catalyst contains 5 wt%  $V_2O_5$  over  $Al_2O_3$ .

### 2.2. Characterization of the catalysts

The BET surface areas of the catalysts were determined on a QUADRASORB SI (Quantachrome Instruments, USA). Prior to nitrogen adsorption at  $-196$  °C, about 100 mg of the sample was degassed at 200 °C for 2 h. A cross-sectional area of  $0.164$  nm<sup>2</sup> of the  $N_2$  molecule was assumed in the calculation of surface area using the Brunauer, Emmett, and Teller (BET) method.

X-ray diffraction patterns of the catalysts were obtained on a Rigaku Miniflex (Rigaku Corporation, Japan) using Ni filtered Cu K $\alpha$  radiation ( $1.5406$  Å) with a scan speed of  $2^\circ$  min<sup>-1</sup> and a scan range of  $10^\circ$ – $80^\circ$  at 30 kV and 15 mA. FT-IR spectra were recorded on a Biorad-Excalibur series (USA) spectrometer using the KBr disc method.

Temperature programmed reduction (TPR) was performed in a flow of 5%  $H_2/Ar$  mixture gas at a flow rate of  $30$  ml min<sup>-1</sup> with a temperature ramp of  $10$  K min<sup>-1</sup>. Prior to the TPR run the catalyst sample (20 mg) was pretreated with argon gas at 250 °C for 2 h. The hydrogen consumption was monitored using a thermal conductivity detector (TCD).

Diffuse reflectance spectra were recorded in the UV-Visible region 200–800 nm at a split width of 1.5 nm and a scan speed of 400 nm per minute using a GBC Cintra 10E UV-Visible spectrometer. Pellets were made by taking 15 mg of the catalyst sample and dried KBr, and grinding them thoroughly for uniform mixing before making the pellets; the spectra were recorded at room temperature.

Temperature programmed desorption of ammonia (TPD- $NH_3$ ) was performed in laboratory built equipment containing a programmable temperature controller and a gas chromatograph with a thermal conductivity detector (TCD). About 100 mg of the catalyst was taken and pretreated at 300 °C for 1 h in He flow ( $30$  ml min<sup>-1</sup>). Then the catalyst was exposed to 10%  $NH_3$  balanced He gas for 1 h at 100 °C. The physisorbed  $NH_3$  was removed under He flow ( $30$  ml min<sup>-1</sup>) for 50 min at the same temperature. Then the temperature of the sample was increased up to 800 °C at a heating rate of  $10$  K min<sup>-1</sup>. The desorbed  $NH_3$  gas was monitored with the gas chromatograph using the thermal conductivity detector.

### 2.3. Catalytic performance

Ammoxidation of 2-chlorotoluene (2-CT) was carried out in a continuous-down flow fixed bed reactor operated under atmospheric pressure. In each catalytic run, about 3 g of the catalyst (crushed to 18/25 BSS sieve to eliminate mass transfer limitations), diluted with double amount of quartz grains, was positioned between two layers of quartz wool at the centre of the reactor. The upper portion of the reactor was filled with quartz beads that served both as a pre-heater and a mixer for

the reactants. Prior to the reaction, the catalyst was reduced with hydrogen ( $60 \text{ ml min}^{-1}$ ) at  $450 \text{ }^\circ\text{C}$  for 2 h. After bringing the reactor temperature to a desired temperature, the reaction feed, with a molar ratio of 2-CT: ammonia: air = 1:4:15, was fed into the preheated portion of the reactor. 2-CT was fed into the reactor through a microprocessor controlled metering pump (B. Braun, Germany). The reaction temperature was monitored using a thermocouple with its tip located at the middle of the catalyst bed. The reactions were carried out in the temperature range of  $360\text{--}450 \text{ }^\circ\text{C}$  with temperature intervals of  $30 \text{ }^\circ\text{C}$ . After allowing the catalyst to attain a steady-state for 1 h at the desired reaction temperature, the liquid product was collected for 30 min in a cold trap kept at  $-10 \text{ }^\circ\text{C}$ . The products were analyzed using a gas chromatograph, separating on a ZB-5 capillary column using a flame ionization detector (FID). From the analysis of the non-condensable exit gas mixture, it was confirmed that the amount of any organic species or oxides of carbon was negligible.

### 3. Results and discussion

#### 3.1. BET specific surface area analysis

Table 1 shows the BET surface area values of  $\text{V}_2\text{O}_5/\text{Al}_2\text{O}_3$  catalysts with varying  $\text{V}_2\text{O}_5$  loadings along with that of the alumina support. The alumina support exhibited a BET surface area of  $205 \text{ m}^2 \text{ g}^{-1}$ . A substantial loss in the BET surface area was observed upon impregnation of  $\text{Al}_2\text{O}_3$  with  $\text{V}_2\text{O}_5$  from 5 to 15 wt%. This is a common phenomenon usually noticed in supported catalysts when the support is impregnated with an active material.<sup>19,25,26</sup> The decrease in surface area after impregnation of vanadia can be ascribed to the penetration of dispersed vanadium oxide species into the pores of alumina which can taper the pore diameter. Alternatively, some of the pores in the support might have been blocked by dispersed vanadia. Besides, the formation of a new species might have been observed by the solid state reaction between dispersed vanadium oxide and the support with a low surface area, as observed from XRD data in the following paragraphs. Similar interpretations have been made in previous reports and the present results are in good agreement with those reports.<sup>25–28</sup>

#### 3.2. Powder X-ray diffraction studies

XRD patterns of the catalysts with various loadings of  $\text{V}_2\text{O}_5$  on  $\text{Al}_2\text{O}_3$  are shown in Fig. 1. Diffractograms of bare  $\text{Al}_2\text{O}_3$  are also provided for the sake of comparison. All the catalysts displayed features indicative of alumina at  $2\theta$  values of  $45.6$  and  $66.6^\circ$  (JCPDS 50-0741). The 5 wt%  $\text{V}_2\text{O}_5/\text{Al}_2\text{O}_3$  catalyst showed

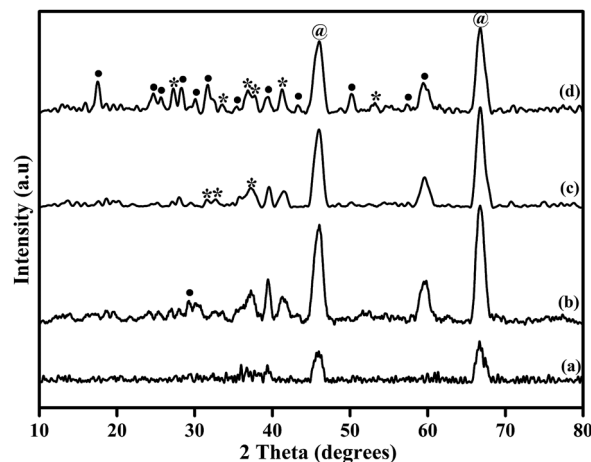


Fig. 1 XRD patterns of the  $\text{V}_2\text{O}_5/\text{Al}_2\text{O}_3$  catalysts: (a)  $\gamma\text{-Al}_2\text{O}_3$ , (b) 5 wt%  $\text{V}_2\text{O}_5/\text{Al}_2\text{O}_3$ , (c) 10 wt%  $\text{V}_2\text{O}_5/\text{Al}_2\text{O}_3$ , (d) 15 wt%  $\text{V}_2\text{O}_5/\text{Al}_2\text{O}_3$ ; (●)  $\gamma\text{-Al}_2\text{O}_3$ , (\*)  $\text{V}_2\text{O}_5$ , (●)  $\text{AlVO}_4$ .

characteristic peaks of  $\text{V}_2\text{O}_5$  and  $\text{AlVO}_4$  with a very low intensity along with those of  $\text{Al}_2\text{O}_3$ . The formation of metal vanadate species (*i.e.*  $\text{AlVO}_4$ ) is very common when  $\text{V}_2\text{O}_5$  is supported on  $\text{Al}_2\text{O}_3$  due to the solid state reaction between dispersed vanadia and alumina. These findings correlate well with the previous literature.<sup>28–31</sup>

Interestingly, the addition of vanadia amplifies the intensity of the characteristic peaks of alumina. From this observation, one can conclude that the addition of  $\text{V}_2\text{O}_5$  enhances the crystallization of  $\text{Al}_2\text{O}_3$ . Klose *et al.*<sup>32</sup> reported that the addition of  $\text{V}_2\text{O}_5$  induces the crystallization of amorphous alumina and also leads to the formation of aluminium vanadate species. A similar observation was also made by Kanervo *et al.*<sup>29</sup> However, the intensity of the characteristic peaks of alumina slightly decreased at higher loadings of  $\text{V}_2\text{O}_5$ , which could be due to the high surface coverage of the support by vanadia and/or also the induced formation of metal vanadates. Meanwhile, only a slight development in the crystalline growth of  $\text{V}_2\text{O}_5$  and  $\text{AlVO}_4$  was observed with the 10 wt%  $\text{V}_2\text{O}_5/\text{Al}_2\text{O}_3$  catalyst, indicating that the vanadia and aluminium vanadate species were in a highly dispersed state. Further addition of  $\text{V}_2\text{O}_5$  to 15 wt% dominated the crystalline formation of aluminium vanadate and vanadia species. Shiju *et al.*<sup>31</sup> studied a  $\text{V}_2\text{O}_5/\text{Al}_2\text{O}_3$  catalytic system by varying the  $\text{V}_2\text{O}_5$  content and found that the vanadia and vanadate species were absent below 10 wt%  $\text{V}_2\text{O}_5$  loading due to the high dispersion of vanadia on alumina with particle sizes lower than the detection limits of XRD and the presence of these species was identified at 20 wt%  $\text{V}_2\text{O}_5$  loading. The present study corroborates the previous reports<sup>28–33</sup> that the formation of microcrystalline  $\text{V}_2\text{O}_5$  and  $\text{AlVO}_4$  starts at 5 wt% loading gradually increasing up to 10 wt% and dominating at 15 wt%  $\text{V}_2\text{O}_5$  loading. These results suggest that the interaction of vanadia with alumina increases from 5 to 10 wt% loading and further addition of  $\text{V}_2\text{O}_5$  to 15 wt% improves the crystalline growth of vanadia and vanadate species. As a consequence of this, the interaction of vanadia with  $\text{Al}_2\text{O}_3$  would be reduced at higher loadings. These results are in good agreement with the

Table 1 BET surface area and total acidity of the support and  $\text{V}_2\text{O}_5/\text{Al}_2\text{O}_3$  catalysts

Catalyst	Surface area ( $\text{m}^2 \text{ g}^{-1}$ )	Total acidity ( $\mu\text{mol g}^{-1}$ )
$\gamma\text{-Al}_2\text{O}_3$	205	321
5 wt% $\text{V}_2\text{O}_5/\text{Al}_2\text{O}_3$	177	1158
10 wt% $\text{V}_2\text{O}_5/\text{Al}_2\text{O}_3$	151	1125
15 wt% $\text{V}_2\text{O}_5/\text{Al}_2\text{O}_3$	125	1071

BET surface area values where a continuous loss in the surface area of the catalysts was observed.

### 3.3. Fourier transform-infrared spectra of the catalysts

Fig. 2 displays the FT-IR spectra of the  $V_2O_5/Al_2O_3$  catalysts with varying  $V_2O_5$  contents along with the support,  $Al_2O_3$ . In the present investigation, 5 and 10 wt%  $V_2O_5/Al_2O_3$  catalysts mainly showed three absorption bands at 1410, 1643, and 3453  $cm^{-1}$ . Additionally, these catalysts also displayed broad absorption bands below 1000  $cm^{-1}$ . From the literature, it is known that crystalline  $V_2O_5$  exhibits bands at 1020, 826 and 609  $cm^{-1}$ . The absorption bands at 1020  $cm^{-1}$  and 826  $cm^{-1}$  can be attributed to the stretching vibrations of the isolated  $V=O$  vanadyl groups in the  $V_2O_5$  trigonal bipyramidal structure and the deformation of the  $V-O-V$  bridges, respectively. The band at 609  $cm^{-1}$  is assignable to bending vibrations.<sup>34–36</sup> The absorption bands of crystalline vanadia below 1000  $cm^{-1}$  were not detected in the present catalysts up to 10 wt%  $V_2O_5$  loading. As the  $Al_2O_3$  support possesses strong IR absorptions below 1000  $cm^{-1}$  due to the ionic character of  $Al-O$  bonds, the bands of crystalline vanadia are obscured.<sup>37</sup>

However, the absorption bands observed at 1643  $cm^{-1}$  and 3453  $cm^{-1}$  are due to the deformation vibrations of adsorbed water and the surface OH groups.<sup>28,38</sup> The intensity of these two bands decreased with the increase in vanadia content from 5 to 10 wt%. Therefore, the possibility of interaction between vanadia and alumina and the formation of polymeric vanadia species cannot be ruled out. The band detected at 1410  $cm^{-1}$  can be related to ammonia formed during the preparation, which remained adsorbed on the catalyst surface even after calcination. To further confirm this absorption band, we treated  $Al_2O_3$  with  $NH_3$  at 450 °C and collected the FT-IR spectrum, which clearly showed an absorption band at 1410  $cm^{-1}$  (Fig. S1, ESI†). 15 wt%  $V_2O_5/Al_2O_3$  displayed three new absorption bands with a very low intensity in the region below 1000  $cm^{-1}$  at 936, 845 and 654  $cm^{-1}$  along with the 1410, 1643, and 3453  $cm^{-1}$  absorption bands. The absorption bands of the ammonium ion, adsorbed

water and surface OH groups decreased considerably in this catalyst due to the possible high surface coverage of alumina by vanadia and/or the involvement of the surface OH groups in polymerization. The appearance of the absorption bands at 845 and 654  $cm^{-1}$  with the 15 wt%  $V_2O_5/Al_2O_3$  catalyst evidently confirms the crystalline nature of vanadia at this loading.<sup>19,32</sup> On the other hand, the band noticed at 936  $cm^{-1}$  ascribed to the  $Al-O-V$  vibrations is a clear indication of the formation of  $AlVO_4$  crystallites by the interaction of vanadia with alumina.<sup>32,39,40</sup> According to Nakagawa *et al.*<sup>41</sup> vanadium oxide on a support surface exists in an amorphous  $V_2O_5$  form at lower loadings, whereas it exists as amorphous and crystalline  $V_2O_5$  or crystalline  $AlVO_4$  at higher loadings. Analogous results were noticed in the present study wherein we observed the absence of the bands corresponding to crystalline vanadia up to 10 wt%  $V_2O_5$  loading, and the apparent presence of the absorption bands of  $V_2O_5$  and  $AlVO_4$  at 15 wt%  $V_2O_5$  loading indeed suggests that the  $V_2O_5$  and  $AlVO_4$  species are in a highly dispersed state up to 10 wt% loading. These findings support the XRD and BET results, where crystalline  $V_2O_5$  and  $AlVO_4$  species were found at higher  $V_2O_5$  loadings in XRD patterns and a substantial decrease in the surface area was observed for catalysts with high vanadia content.

### 3.4. $H_2$ -Temperature programmed reduction studies

TPR is a highly useful technique to characterize the redox properties of different metal oxides. TPR profiles of  $V_2O_5/Al_2O_3$  catalysts with varying  $V_2O_5$  contents are presented in Fig. 3. Both 5 and 10 wt%  $V_2O_5/Al_2O_3$  catalysts showed a single broad reduction peak in the temperature region of 420–731 °C with  $T_{max}$  at 605 and 637 °C, respectively. The 15 wt%  $V_2O_5/Al_2O_3$  catalyst mainly exhibited a broad reduction peak in the region of 485–676 °C with  $T_{max}$  at 608 °C. This catalyst also displayed a small and broad reduction peak in the region of 374–480 °C with  $T_{max}$  at 436 °C. The single reduction peak observed in the present study is in good accordance with previous reports.<sup>25,28,31,32,42–45</sup> The single peak was found for reported catalysts<sup>46,47</sup> with less

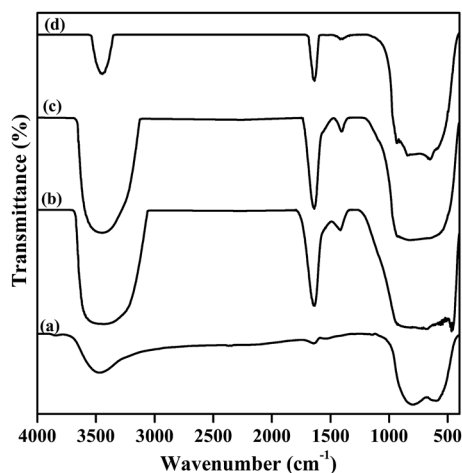


Fig. 2 FT-infrared spectra of the  $V_2O_5/Al_2O_3$  catalysts: (a)  $\gamma$ - $Al_2O_3$ , (b) 5 wt%  $V_2O_5/Al_2O_3$ , (c) 10 wt%  $V_2O_5/Al_2O_3$ , and (d) 15 wt%  $V_2O_5/Al_2O_3$ .

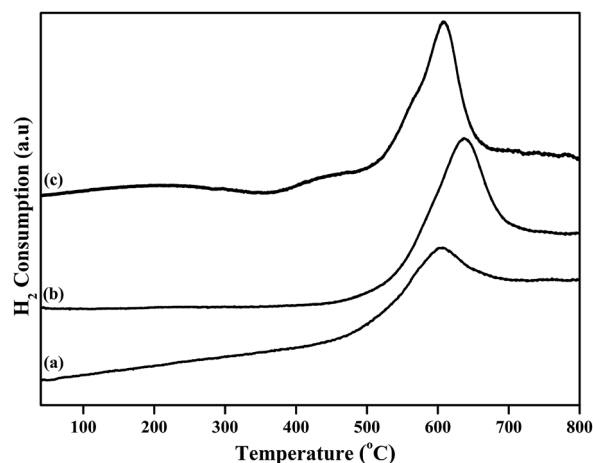


Fig. 3 TPR profiles of the  $V_2O_5/Al_2O_3$  catalysts: (a) 5 wt%  $V_2O_5/Al_2O_3$ , (b) 10 wt%  $V_2O_5/Al_2O_3$ , and (c) 15 wt%  $V_2O_5/Al_2O_3$ .

than four layers of  $V_2O_5$  deposited on the support. However, with the formation of a single peak, it is difficult to distinguish the different kinds of vanadium oxide species formed on  $Al_2O_3$ .

It is well-known that the textural properties of support materials (*e.g.*, surface area, porosity), impurities (foreign compounds), and preparation method, and calcination temperature play an important role in the reducibility of vanadia. In addition to these the reduction temperature is also sensitive to the reduction conditions, such as  $H_2$  partial pressure and heating rate. Therefore, it is difficult to identify a common feature for the reduction of catalysts. For example, Xiang *et al.*<sup>44</sup> studied various supported vanadium catalysts and reported that 5 V/nano- $Al_2O_3$  was reduced at 569 °C, whereas 5 V/com- $Al_2O_3$  was reduced at 552 °C, suggesting that the interactions of vanadia and nano- $Al_2O_3$  were stronger than those of vanadia and com- $Al_2O_3$ . Chen *et al.*,<sup>45</sup> in their study on  $V_2O_5/Al_2O_3$  catalysts, observed a single reduction peak in the range of 500–520 °C below a vanadium loading of 1.50 mmol  $g^{-1}$ - $Al_2O_3$ , while two reduction peaks were found, one at around 530–550 °C and the other at 625 °C at higher loadings of vanadia. The reduction peak noticed at lower temperature was attributed to the isolated surface vanadia species while the high temperature one was due to the reduction of the polymeric vanadia species. da Silva *et al.*<sup>42</sup> reported a broad and intense reduction peak at 638 °C with a small shoulder at 777 °C for a  $V_2O_5/Al_2O_3$  catalyst. The vanadia species reduced at 638 °C belonged to the polymeric vanadia species while the vanadia species reduced at 777 °C was the monovanadate ( $V=O$ ) species. Ferreira and Volpe,<sup>48</sup> in their theoretical and experimental study of supported vanadium catalysts, revealed that the structure, coordination and  $VO_x$ -support interaction were strongly influenced by the nature of support. From the calculations of stabilization and formation energies, they found that the presence of dimeric vanadia species on  $SiO_2$  supports was ruled out, while  $V(=O)_2$  and  $V=O$  species were the most plausible species. The dimeric vanadia species were most conceivable on  $Al_2O_3$  and  $TiO_2$  supports.

It was acknowledged from previous studies<sup>28,45,48,49</sup> that the isolated surface vanadia species easily underwent reduction than polymeric or bulk like  $V_2O_5$  species. Thus, from the TPR results, one can conclude that the  $T_{max}$  observed at 605 °C for the 5 wt%  $V_2O_5/Al_2O_3$  catalyst is due to the reduction of the polymeric vanadia species (*i.e.*  $V^{5+}$  to  $V^{4+}$ ). At 10 wt%  $V_2O_5$  loading, the  $T_{max}$  shifts towards higher temperature (*i.e.* 637 °C) with a greater intensity. The improved intensity with the high temperature shift indicates the induced formation of the polymeric vanadia species. This also suggests a strong interaction between polymeric vanadia and  $Al_2O_3$ . But one cannot rule out the presence of isolated surface vanadia species in 5 and 10 wt%  $V_2O_5$  catalysts. In the case of the 15 wt% catalyst, the reduction profile had changed significantly. This is due to the formation of isolated surface vanadia species (*i.e.* low temperature peak) along with polymeric vanadia species (*i.e.* high temperature peak). But one cannot ignore the reduction of  $AlVO_4$  which can be seen between 480–650 °C<sup>29</sup>, whose formation is dominant in the 15 wt%  $V_2O_5/Al_2O_3$  catalyst which is known from the XRD results. Hence, the  $T_{max}$  shift found at a

higher temperature in the 15 wt%  $V_2O_5/Al_2O_3$  catalyst is due to the presence of crystalline  $AlVO_4$  in conjunction with a decrease in the interaction of the polymeric vanadia species with alumina. The TPR results support the XRD and FT-IR data, in which crystalline  $V_2O_5$  species was found at higher loadings. From the TPR results, one can conclude that the isolated surface vanadia and polymeric vanadia species are in a highly dispersed state and/or having a strong interaction with the  $Al_2O_3$  support up to 10 wt%  $V_2O_5$  loading and their interaction decreases considerably at 15 wt%  $V_2O_5$  loading.

### 3.5. UV-Vis diffuse reflectance spectra of the catalysts

UV-Vis diffuse reflectance spectra of the catalysts with various loadings of  $V_2O_5$  on  $Al_2O_3$  are depicted in Fig. 4. It is known that the energy of the oxygen to vanadium charge transfer (LMCT) absorption band is strongly influenced by the number of oxygen ligands surrounding the central vanadium ion. This information can be used to determine the nature of the coordination of vanadium ions in different types of surface species.<sup>50–52</sup> According to previous reports,<sup>50–54</sup> vanadium can be distributed on supports with the formation of different kinds of species *i.e.* tetrahedrally coordinated monomeric or isolated vanadia species and small clusters or linear chains usually observed at absorption maxima around 230–250 nm. The oligo or polymeric vanadia species formed by the condensation of monomeric vanadia species are found at around 270–300 nm, by retaining the tetrahedral coordination geometry. The band observed at 400 nm is related to the vanadium ion surrounded by a square pyramid of five oxygen ligands, with a distant sixth ligand in a bridging position to the support. These species, generated by a two-dimensional condensation reaction of immobilized vanadia, can also be present as ribbons, patches or two-dimensional surface layers. The absorption bands of  $V^{5+}$  falling in the 430–570 nm region are characteristic of distorted octahedral coordination or bulk-like vanadia crystallites. The d–d transitions of  $V^{4+}$  and  $V^{3+}$  ions appear at above 570 nm.

All the catalysts in the present study exhibited broad absorption bands lying in the region of 200–475 nm. The appearance

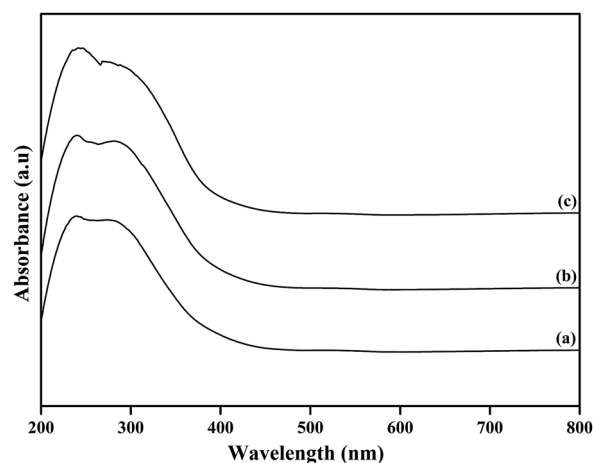


Fig. 4 UV-Vis DR spectra of the  $V_2O_5/Al_2O_3$  catalysts: (a) 5 wt%  $V_2O_5/Al_2O_3$ , (b) 10 wt%  $V_2O_5/Al_2O_3$ , and (c) 15 wt%  $V_2O_5/Al_2O_3$ .

of a broad band in all the catalysts indicates the presence of different kinds of vanadium species. The 5 wt%  $V_2O_5/Al_2O_3$  catalyst showed two absorption maxima at 238 and 278 nm, respectively. In the case of the 10 wt%  $V_2O_5/Al_2O_3$  catalyst, there is a tiny red shift in both the absorption bands towards the higher wavelength (*i.e.* 239 and 282 nm) with an improved intensity. A noticeable change was observed in 15 wt%  $V_2O_5/Al_2O_3$ . The red shift now occurred at 243 and 286 nm. Very often, literature reports on this subject assign these absorption bands based on the changes in the coordination and/or polymerization degree of vanadium atoms. Following this criterion, the former absorption band observed at around 238–243 nm can be ascribed to the monomeric or isolated tetrahedral vanadia species while the latter absorption band perceived in the region of 278–286 nm can be assigned to the polymeric tetrahedral vanadia species.<sup>50–54</sup>

According to the investigations of Shiju *et al.*<sup>31</sup> and Khodakov *et al.*,<sup>33</sup> vanadia dispersed on alumina shows a broad range of  $VO_x$  structures. They suggested that  $V_2O_5$  predominantly exists as monomeric or isolated vanadia species with tetrahedral coordination at lower loadings while polymeric vanadia species are observed at higher loadings due to progressive condensation of the monomeric species. Besides, bulk-like  $V_2O_5$  crystallites were noticed at above 20 wt%  $V_2O_5$  loadings. Xiang *et al.*<sup>44</sup> and Liu *et al.*<sup>55</sup> observed a broad absorption band at 300 nm which was indicative of polymeric vanadia species. They found a new absorption band at 450 nm for the catalyst with 25 wt%  $V_2O_5$  loading, suggesting the formation of bulk-like vanadia crystallites due to further polymerization of the vanadia species. Similar views were also expressed in the literature<sup>31,33,44,55,56</sup> stating that the appearance of a broad band at higher wavelengths for the catalysts with high loadings of  $V_2O_5$  is due to the growth in size and dimensionality of vanadia species. In the present investigation, the absorption profiles, showing an increase in the intensity of both absorption bands with the addition of  $V_2O_5$  and the red shift, are indicative of an increase in the degree of vanadium condensation resulting in the formation of the polymeric vanadia species. These findings correlate with previous reports<sup>31,57</sup> and are also in good agreement with the FT-IR results, where we found a decrease in the intensity of the surface OH region due to the polymerization. The broadness of the absorption bands also indicates the growth of the crystalline vanadia species. The absence of the absorption band in the visible region suggests the absence of the d-d transitions of the  $V^{4+}$  and  $V^{3+}$  ions.

### 3.6. Temperature programmed desorption of $NH_3$

The  $NH_3$ -TPD profiles of the catalysts are presented in Fig. 5, and the total acidity values of the catalysts are given in Table 1. The  $Al_2O_3$  support showed two desorption peaks centered at 200 and 655 °C indicating that alumina had both weak and strong acidic sites with a total acidity of 321  $\mu\text{mol g}^{-1}$ .<sup>58</sup> In general, the acid site distribution observed from the  $NH_3$ -TPD studies can be differentiated into three temperature regions *viz.* 100–350 °C (weak acidic sites), 350–600 °C (moderate acidic sites) and above 600 °C (strong acidic sites).

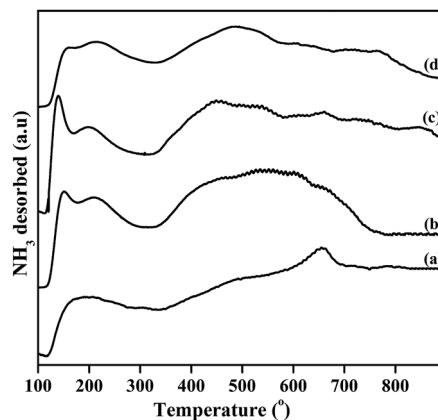


Fig. 5  $NH_3$ -TPD profiles of the  $V_2O_5/Al_2O_3$  catalysts: (a)  $\gamma$ - $Al_2O_3$  (b) 5 wt%  $V_2O_5/Al_2O_3$ , (c) 10 wt%  $V_2O_5/Al_2O_3$ , and (d) 15 wt%  $V_2O_5/Al_2O_3$ .

All the  $V_2O_5/Al_2O_3$  catalysts clearly exhibited two broad desorption peaks except for the 15 wt%  $V_2O_5/Al_2O_3$  catalyst, in which three broad desorption peaks were noticed. It is noteworthy that the first desorption peak appearing in the low temperature region *i.e.* below 350 °C in all the catalysts splits into two peaks with  $T_{max}$  lying in the temperature ranges of 140–160 °C and 200–215 °C, respectively. In the 5 wt%  $V_2O_5/Al_2O_3$  catalyst, these two peaks were identified at 150 °C and 210 °C. The  $T_{max}$  values shifted to a lower temperature in the 10 wt%  $V_2O_5/Al_2O_3$  catalyst and were observed at 140 and 200 °C. These  $T_{max}$  values moved to a higher temperature and were detected at 160 and 215 °C in the 15 wt%  $V_2O_5/Al_2O_3$  catalyst. The desorption peak seen at 140–160 °C can be ascribed to the isolated surface vanadia species and the latter visible at 200–215 °C can be attributed to the Lewis acidity of uncovered alumina. The broad desorption peak appearing above 350 °C is due to the Bronsted acidity of the highly dispersed and/or polymeric vanadia species.<sup>58–60</sup> The broadness of the second peak extending to a higher temperature is separated into two desorption peaks in the case of high  $V_2O_5$  loadings.

Khader<sup>59</sup> studied the surface acidity of  $V_2O_5/Al_2O_3$  catalysts by IR and TPD. The  $V_2O_5/Al_2O_3$  catalyst showed Bronsted acidity due to V–OH species while Lewis acidity corresponded to the uncovered Al ions at lower vanadia loadings. He also suggested that the Lewis acidity of the monolayer catalyst was caused by the isolated surface vanadia species. Nonetheless, at higher loadings of vanadia, the Bronsted acidity of the catalysts was prominent due to two kinds of vanadia species *i.e.* the V–OH species of adsorbed vanadium oxide on alumina and the V–OH species of crystalline  $V_2O_5$ . However, the decrease in the Lewis acidity at higher loadings of  $V_2O_5$  is due to the surface coverage of crystalline  $V_2O_5$  and/or decrease in the number of OH groups attached to the vanadium atoms due to the consumption of the V–OH species during polymerization. Miyata *et al.*<sup>61</sup> mentioned that the Bronsted acidic sites of monolayer or two-dimensional or polymeric vanadia species are stronger than those obtained in higher vanadia loadings due to crystalline  $V_2O_5$ .

The 5 wt%  $V_2O_5/Al_2O_3$  catalyst exhibited approximately four fold higher acidity (*i.e.* 1158  $\mu\text{mol g}^{-1}$ ) than the pure support.

Such kind of massive enrichment in the catalyst acidity can be caused by the formation of polymeric vanadia species on the support. There was no significant decrease in the acidity with the addition of  $V_2O_5$  up to 10 wt%. A substantial decrease in the acidity was noticed for 15 wt%  $V_2O_5/Al_2O_3$ . The observed results can be easily understood from the XRD, FT-IR, TPR and UV-Vis DRS information. All these studies recommended the crystalline growth of vanadia species as a result of increased polymerization of the vanadia species from 5 to 15 wt%  $V_2O_5$  loading. The apparent enhancement of the low temperature peak intensity and the broadness of the peak at a high temperature in the 10 wt%  $V_2O_5/Al_2O_3$  catalyst was due to the induced formation of isolated and polymeric vanadia species. The appearance of three desorption peaks at low, moderate and high temperatures in the 15 wt%  $V_2O_5/Al_2O_3$  catalyst can be described as follows: the low temperature desorption peak is due to the isolated surface vanadia species and uncovered alumina, the moderate temperature desorption peak is ascribed to the V-OH species of crystalline  $V_2O_5$  and the high temperature desorption is due to the V-OH species of polymeric vanadia. These results are in good agreement with previous reports.<sup>59,61</sup> The significant fall in the acidity of the 15 wt%  $V_2O_5/Al_2O_3$  catalyst is due to the formation of the crystalline vanadia and vanadate species.

### 3.7. Ammoxidation of 2-chlorotoluene (2-CT)

All these catalytic systems were used for the evaluation of ammoxidation of 2-chlorotoluene (2-CT) in a fixed bed reactor at atmospheric pressure. The main product obtained in the ammoxidation of 2-CT was 2-chlorobenzonitrile (2-CBN). Due to the exothermic nature, the formation of by-products is very common in ammoxidation reactions. The usual by-products seen in the ammoxidation of 2-CT are as follows: chloro-benzene (due to loss of methyl group) and carbon oxides (*i.e.* CO and  $CO_2$ , due to the partial, total oxidation of methyl group/2-CT). However, in the present study, we did not find the formation of any by-products and observed the exclusive formation of the desired product, 2-CBN.

#### 3.7a. Effect of $V_2O_5$ content on the catalytic activity.

Ammoxidation of 2-CT was carried out over  $V_2O_5/Al_2O_3$  catalysts in order to study the variation in catalytic activity as a function of  $V_2O_5$  content at 420 °C and the results are depicted in Fig. 6. Irrespective of  $V_2O_5$  loading, all the catalysts showed 100% selectivity towards a single product *i.e.* 2-CBN. No other by-product was detected. A considerable variation in the 2-CT conversion was observed with respect to the  $V_2O_5$  loading. The 5 wt%  $V_2O_5/Al_2O_3$  catalyst showed only 28% conversion. However, progress in the catalytic activity was noticed with the addition of  $V_2O_5$ . The 10 wt% catalyst achieved higher catalytic activity with 41% conversion. A further increase in the active component to 15 wt% decreased the conversion and it reached a value of 35%. The difference noticed in the catalytic activity can be correlated with the observed characteristics of the catalysts.

The lower catalytic activity acquired by the 5 wt%  $V_2O_5/Al_2O_3$  catalyst can be due to the low content of  $V_2O_5$ . But the 10 wt%  $V_2O_5/Al_2O_3$  catalyst achieved the highest catalytic activity

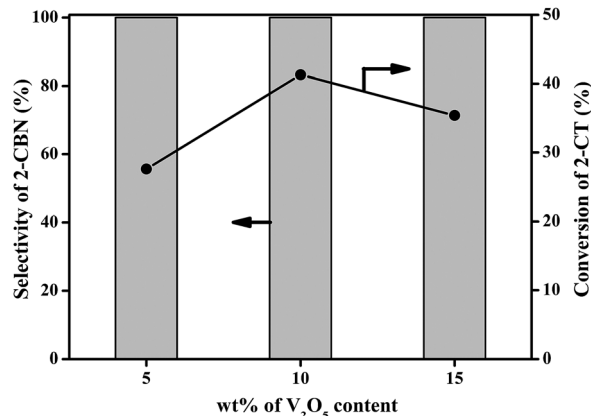


Fig. 6 Effect of  $V_2O_5$  loading on the catalytic activity of the ammoxidation of 2-CT at 420 °C.

among the series of catalysts. Such kind of huge improvement in the catalytic activity can be conceivable, due to the induced formation of the isolated surface and polymeric vanadia species, which in turn result in a stronger interaction with the support  $Al_2O_3$ . The noticed decrease in the catalytic activity of the 15 wt%  $V_2O_5/Al_2O_3$  catalyst was due to the enormous formation of crystalline  $V_2O_5$  and  $AlVO_4$  and a subsequent loss in the highly dispersed and/or polymeric vanadia species. These results are in good agreement with the previous literature.<sup>19</sup>

It is well known from the literature<sup>62,63</sup> that metal vanadates are active and selective catalysts for ammoxidation reactions. Dhachapally *et al.*<sup>62</sup> carried out ammoxidation of 2-methylpyrazine over metal vanadate catalysts and observed that the  $AlVO_4$  catalyst showed higher catalytic activity. They also mentioned that a small proportion of crystalline  $V_2O_5$  species in the catalysts are also beneficial for ammoxidation reactions. In addition, the acidity of the catalysts also plays a decisive role in the ammoxidation reaction by the way of enhancing the absorption capacity of one of the reactants, ammonia. From  $NH_3$ -TPD studies, it was noted that only a small difference in acidity was perceived between the 5 and 10 wt%  $V_2O_5/Al_2O_3$  catalysts. However, a large disparity in the acidity was noticed in the 15 wt%  $V_2O_5/Al_2O_3$  catalyst due to the low availability of the surface OH groups as they were involved in the polymerization, which ultimately led to the formation of crystalline  $V_2O_5$ . These results suggest that 10 wt%  $V_2O_5/Al_2O_3$  is the best catalyst among the catalytic systems studied due to the induced formation of isolated surface and polymeric vanadia species with reasonable acidity. Besides, the presence of small proportions of crystalline  $V_2O_5$  and  $AlVO_4$  species is favorable to obtain high catalytic activity.

**3.7b. Effect of temperature on the catalytic activity.** The effect of the reaction temperature on the catalytic activity of the 10 wt%  $V_2O_5/Al_2O_3$  catalyst is projected in Fig. 7. It is obvious that the conversion of 2-CT increases with an increase in the reaction temperature from 360 to 450 °C. The conversion of 2-CT was two fold when the temperature increased from 360 to 390 °C. A further increase in the temperature enhanced the conversion of 2-CT and the maximum conversion was attained

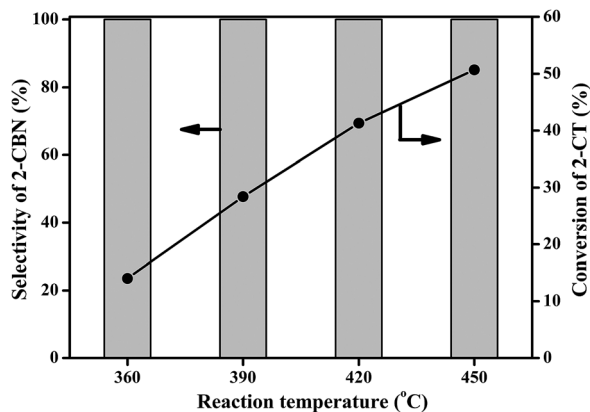


Fig. 7 Effect of the reaction temperature on the catalytic activity of the 10 wt%  $V_2O_5/Al_2O_3$  catalyst in the ammoxidation of 2-CT.

at 450 °C *i.e.* 51%. All the catalysts gave only one product, 2-CBN, at every temperature without the formation of any byproduct. Dhachapally *et al.*<sup>63</sup> and Kung *et al.*<sup>64,65</sup> reported that metal vanadates have lower combustion activity than  $V_2O_5$ , which is reflected in showing high selectivity towards the desired product even at higher temperatures. Owen and Kung<sup>64</sup> used different metal vanadates for the ODH of butane and suggested that orthovanadate materials exhibit high selectivity towards the desired product, wherein the  $VO_4$  units are separated from each other by  $MO_x$  units. In such materials, most of the lattice oxygen ions are located in the solid bridge between the  $V^{5+}$  and  $M^{2+}$  ions resulting in low availability of readily removable lattice oxygen, which leads to low combustion or total oxidation.

Recently, Dhachapally *et al.*<sup>66</sup> recounted that oligomeric/polymeric vanadia species are considered to be selective for the formation of 2-cyanopyrazine during ammoxidation of 2-methylpyrazine. Similarly, Bilde *et al.*<sup>67</sup> recommended that the presence of isolated surface vanadia species or of low size oligomeric vanadium oxide species in the catalysts was responsible for the higher selectivity of acrylonitrile in the ammoxidation of propane. In the present study, all the catalysts possess isolated surface and polymeric vanadia species along with the aluminum vanadate species. As a result, these catalysts selectively yielded 2-CBN as the product in the ammoxidation of 2-CT even at higher temperatures. To further confirm that the isolated surface vanadia, polymeric vanadia and aluminum vanadate species were responsible for the selectivity of 2-CBN, ammoxidation was carried out on 20 and 25 wt%  $V_2O_5/Al_2O_3$  catalysts which possess more crystalline  $V_2O_5$  and  $AlVO_4$  than the studied catalysts (see Fig. S2 in ESI† for XRD). These catalysts yielded around 40 and 36% of 2-CT conversion with 97% selectivity towards 2-CBN at 450 °C. The observed variation in the ammoxidation activity could be associated with the difference in the crystallinity of the catalysts. These results are well corroborated by the previous literature.<sup>19</sup> In addition, these catalysts exhibited lower selectivity than the studied catalysts due to transformation of most of the isolated and polymeric vanadia species into more crystalline  $V_2O_5$  and  $AlVO_4$ . But they still showed the highest selectivity to 2-CBN due to the presence of a

large amount of crystalline  $AlVO_4$ , which is known to have lower combustion activity than  $V_2O_5$ .<sup>63–65</sup> Hence, these results further confirm that bulk and crystalline  $V_2O_5$  are detrimental for high product selectivity whereas isolated surface vanadia, polymeric vanadia and aluminum vanadate species are accountable for the high selectivity towards 2-CBN. Therefore, from these results one can conclude that vanadia catalysts with a high content of isolated surface and polymeric tetrahedral vanadia species with reasonable acidity can exhibit considerable activity and high selectivity in ammoxidation reactions. More to the point, the presence of small grains of  $V_2O_5$  and  $AlVO_4$  species is always crucial in these catalysts to attain higher catalytic activity along with selectivity.

Herein, we discussed the mechanistic aspects reported in the literature using  $Al_2O_3$  supported  $V_2O_5$  catalysts for the ammoxidation of toluene and 2-chlorotoluene. Murakami *et al.*<sup>12</sup> and Niwa *et al.*<sup>68</sup> investigated the reaction mechanism of ammoxidation of toluene using  $V_2O_5/Al_2O_3$  catalysts by FTIR spectroscopy. They claimed that the reaction proceeds by the interaction of ammonium ions with surface benzoate ions. Otamiri and Andersson<sup>69</sup> proposed the formation of vanadium imido species ( $V=NH$ ) and vanadium hydroxylamino species ( $V-NH-OH$ ) as nitrogen insertion sites in  $V_2O_5$  catalysts. These species, in turn, reacted with adsorbed toluene to form an amine ( $R-CH_2-NH_2$ ) and/or an imine ( $R-CH=NH$ ) surface intermediate, which then transformed into nitrile as the final product. Very recently, Dwivedi *et al.*<sup>19</sup> proposed a mechanism for ammoxidation of 2-CT to 2-CBN over  $Al_2O_3$  supported  $V_2O_5$  catalysts using DFT computations. According to their study, the  $V_2O_5/Al_2O_3$  catalyst was first reduced by  $NH_3$  to form vanadium imido ( $V=NH$ ) species and then a 2-CT molecule would adsorb through a vanadyl oxygen ( $V=O$ ) to produce  $C_6H_5=CH_2$  species. Subsequently, the formed  $C_6H_5=CH_2$  species was adsorbed on the vanadium imido ( $V=NH$ ) species to produce 2-CBN *via* three successive dehydrogenation steps. For the DFT calculations, they used four-coordinated alumina supported polymeric vanadium oxide as the active species, and the catalytic systems of the present study are composed of these species and thus follow the same reaction pathways.

It is well-known that ammoxidation reactions of methyl aromatics follow a redox mechanism as proposed by Mars and van Krevelen.<sup>70</sup> According to this mechanism, lattice oxygen is consumed in the reaction and the reduced site formed would be reoxidized by gaseous oxygen. Hence, the reduction of vanadium based catalysts is always pursued prior to the ammoxidation reaction to generate more coordinatively unsaturated sites ( $V^{4+}$ ), which facilitate the redox mechanism ( $V^{4+}/V^{5+}$ ) and in turn the ammoxidation activity. Another important point to be considered in almost all ammoxidation reactions is ammonia oxidation. There is always a competition between  $NH_3$  oxidation, and ammoxidation on the catalyst surface. Moreover, the contact of ammonia with the catalyst surface, particularly at high temperatures, causes a partial reduction of the oxide surface due to the occurrence of  $NH_3$  oxidation. Therefore, control of the rate of unselective oxidation of ammonia to  $N_2$  ( $NO_x$ )<sup>71,72</sup> is an important factor in determining the selectivity of the nitrile product in the

ammonoxidation reaction, because this side reaction limits the availability of surface ammonia (N-insertion) species that are necessary for nitrile formation. It is known from the literature<sup>71,72</sup> that the oxidation of ammonia is faster than the ammonoxidation reaction; excess ammonia modifies the surface oxidation characteristics of a catalyst and decreases the ammonoxidation activity. Nevertheless, it is also very difficult to completely avoid ammonia oxidation but it can only be minimised to the maximum possible extent. Besides, coordinatively unsaturated sites act as Lewis acidic sites for the chemisorption of methyl aromatics and NH<sub>3</sub>. On the other hand, the acidity of the catalyst plays a critical role in the ammonoxidation reaction. It is obvious that enhanced acidity is favourable for the better performance of catalysts as it is known that NH<sub>3</sub> can adsorb on the catalyst surface in the form of either NH<sub>4</sub><sup>+</sup> on Bronsted acid sites or coordinatively adsorbed NH<sub>3</sub> on Lewis acid sites. The mode of adsorption of NH<sub>3</sub>, however, depends on the various parameters such as temperature, hydroxylation state of the catalyst, etc.<sup>72</sup> But the strong acidity of the catalyst always leads to the formation of undesired products such as de-methylated products and carbon oxides due to the strong adsorption of methyl aromatic compounds. Hence, it is indispensable to maintain a good balance between the redox and acidic properties to attain high ammonoxidation activity and selectivity.

## 4. Conclusions

Al<sub>2</sub>O<sub>3</sub> supported V<sub>2</sub>O<sub>5</sub> catalysts are active and selective for the one-step synthesis of 2-chlorobenzonitrile from 2-chlorotoluene *via* ammonoxidation. Both vanadia content and reaction temperature have a strong influence on the ammonoxidation activity. An increase in V<sub>2</sub>O<sub>5</sub> beyond 5 wt% increases the crystallinity of amorphous alumina and causes the formation of aluminium vanadate species. Vanadia can exist in the catalysts in the form of isolated surface and polymeric tetrahedral vanadia species. Their formation is influenced by the vanadia content present in the catalyst. The high selectivity of 2-CBN can be due to the formation of the isolated surface and polymeric tetrahedral vanadia species along with the aluminium vanadate species. The 10 wt% V<sub>2</sub>O<sub>5</sub>/Al<sub>2</sub>O<sub>3</sub> catalyst is the best among the catalytic systems studied, due to the induced formation of isolated surface and polymeric tetrahedral vanadia species having reasonable acidity. Small proportions of crystalline V<sub>2</sub>O<sub>5</sub> and AlVO<sub>4</sub> species are also beneficial to achieve high catalytic activity. Further efforts are very much needed to understand the role of tetrahedral and octahedral coordination geometry of vanadia species on the activity and selectivity in ammonoxidation reactions.

## Conflicts of interest

There are no conflicts to declare.

## Acknowledgements

The authors gratefully thank the Council of Scientific and Industrial Research (CSIR), India, for financial support. This research

was also financially supported by the Basic Science Research Program through the National Research Foundation of Korea (NRF) funded by the Ministry of Education, Republic of Korea (NRF-2016R1A6A1A03013422).

## References

- 1 B. M. Weckhuysen and D. E. Keller, *Catal. Today*, 2003, **78**, 25–46.
- 2 Y. Zhao, Z. Qin, G. Wang, M. Dong, L. Huang, Z. Wu, W. Fan and J. Wang, *Fuel*, 2013, **104**, 22–27.
- 3 D. Gazzolia, S. D. Rossi, G. Ferraris, G. Mattei, R. Spinicci and M. Valigi, *J. Mol. Catal. A: Chem.*, 2009, **310**, 17–23.
- 4 P. Forzatti, *Appl. Catal., A*, 2001, **222**, 221–236.
- 5 K. V. R. Chary, G. Kishan, T. Bhaskar and Ch. Sivaraj, *J. Phys. Chem. B*, 1998, **102**, 6792–6798.
- 6 Y. Jeon, S. W. Row, A. Dorjgotov, S. D. Lee, K. Oh and Y. G. Shul, *Korean J. Chem. Eng.*, 2013, **30**, 1566–1570.
- 7 A. A. Lemonidou, L. Nalbandian and I. A. Vasalos, *Catal. Today*, 2000, **61**, 333–341.
- 8 G. Bergeret, P. Gallezot, K. V. R. Chary, B. R. Rao and V. S. Subrahmanyam, *Appl. Catal.*, 1988, **40**, 191–196.
- 9 J. Haber, A. Kozłowska and R. Kozłowski, *J. Catal.*, 1989, **102**, 52–63.
- 10 J. G. Eon, R. Olier and J. C. Volta, *J. Catal.*, 1994, **145**, 318–326.
- 11 M. Sanati, A. Andersson, L. R. Wallenberg and B. Rebenstorff, *Appl. Catal., A*, 1993, **106**, 51–72.
- 12 Y. Murakami, M. Niwa, T. Hattori, S. Osawa, I. Igushi and H. Ando, *J. Catal.*, 1977, **49**, 83–91.
- 13 B. N. Reddy, B. M. Reddy and M. Subrahmanyam, *J. Chem. Soc., Chem. Commun.*, 1988, 33–34.
- 14 B. N. Reddy, B. M. Reddy and M. Subrahmanyam, *J. Chem. Soc., Faraday Trans.*, 1991, **87**, 1649–1655.
- 15 N. Dropka, V. N. Kalevaru, A. Martin, D. Linke and B. Lucke, *J. Catal.*, 2006, **240**, 8–17.
- 16 V. N. Kalevaru, B. Lucke and A. Martin, *Catal. Today*, 2009, **142**, 158–164.
- 17 X. G. Yong and H. Chi, *Indian J. Chem. Technol.*, 2007, **14**, 371–375.
- 18 B. H. Babu, K. T. V. Rao, M. Surendar, P. S. S. Prasad and N. Lingaiah, *React. Kinet., Mech. Catal.*, 2015, **114**, 121–134.
- 19 R. Dwivedi, P. Sharma, A. Sisodiya, M. S. Batra and R. Prasad, *J. Catal.*, 2017, **345**, 245–257.
- 20 V. Krishnan, T. Raju, A. Muthukumaran and K. Kulangiappar, *Indian Pat.*, 230374, 2009.
- 21 A. Martin and B. Lucke, *Catal. Today*, 1996, **32**, 279–283.
- 22 A. Martin, B. Lucke, H. Seeboth, G. Ladwig and E. Fischer, *React. Kinet. Catal. Lett.*, 1989, **38**, 33–38.
- 23 A. Martin, B. Lucke, G. U. Wolf and M. Meisel, *Catal. Lett.*, 1995, **33**, 349–355.
- 24 Z. Qiong, H. Chi, G. Xie, C. Xu and Y. Chen, *Synth. Commun.*, 1999, **29**, 2349–2353.
- 25 S. A. Ghamdi, M. Volpe, M. M. Hossain and H. de Lasa, *Appl. Catal., A*, 2013, **450**, 120–130.

- 26 G. C. Bond and S. F. Tahir, *Appl. Catal.*, 1991, **71**, 1–31.
- 27 B. M. Reddy, P. Lakshmanan and A. Khan, *J. Phys. Chem. B*, 2004, **108**, 16855–16863.
- 28 E. P. Reddy and R. S. Varma, *J. Catal.*, 2004, **221**, 93–101.
- 29 J. M. Kanervo, M. E. Harlin, A. Outi, I. Krause and M. A. Bañares, *Catal. Today*, 2003, **78**, 171–180.
- 30 I. Baldychev, R. J. Gorte and J. M. Vohs, *J. Catal.*, 2010, **269**, 397–403.
- 31 N. R. Shiju, M. Anilkumar, S. P. Mirajkar, C. S. Gopinath, B. S. Rao and C. V. Satyanarayana, *J. Catal.*, 2005, **230**, 484–492.
- 32 F. Klose, T. Wolff, H. Lorenz, A. S. Morgenstern, Y. Suchorski, M. Piórkowska and H. Weiss, *J. Catal.*, 2007, **247**, 176–193.
- 33 A. Khodakov, B. Olthof, A. T. Bell and E. Iglesia, *J. Catal.*, 1999, **181**, 205–216.
- 34 V. V. Kaichev, G. Y. Popova, Y. A. Chesalov, A. A. Saraev, D. Y. Zemlyanov, S. A. Beloshapkin, A. K. Gericke, R. Schlögl, T. V. Andrushkevich and V. I. Bukhtiyarov, *J. Catal.*, 2014, **311**, 59–70.
- 35 V. Dimitrov, Y. Dimitriev and A. Montenero, *J. Non-Cryst. Solids*, 1994, **180**, 51–57.
- 36 B. P. Barbero and L. E. Cadus, *Appl. Catal.*, A, 2003, **244**, 235–249.
- 37 M. A. Vuurman, D. J. Stufkens, A. Oskam, G. Deo and I. E. Wachs, *J. Chem. Soc., Faraday Trans.*, 1996, **92**, 3259–3265.
- 38 K. V. Narayana, A. Venugopal, K. S. R. Rao, S. K. Masthan, V. V. Rao and R. K. Rao, *Appl. Catal.*, A, 1998, **167**, 11–22.
- 39 N. Magg, B. Immaraporn, J. B. Giorgi, T. Schroeder, M. Bäumer, J. Döbler, Z. Wu, E. Kondratenko, M. Cherian, M. Baerns, P. C. Stair, J. Sauer and H. J. Freund, *J. Catal.*, 2004, **226**, 88–100.
- 40 N. Magg, J. B. Giorgi, T. Schroeder, M. Bäumer and H. J. Freund, *J. Phys. Chem. B*, 2002, **106**, 8756–8761.
- 41 Y. Nakagawa, O. Ono, H. Miyata and Y. Kubokawa, *J. Chem. Soc., Faraday Trans.*, 1983, **79**, 2929–2936.
- 42 T. C. da Silva, E. B. Pereira, R. P. dos Santos, B. Louis, J. P. Tessonnier and M. M. Pereira, *Appl. Catal.*, A, 2013, **462–463**, 46–55.
- 43 A. W. S. Kreemers, G. C. V. Leerdam, J. P. Jacobs, H. H. Brongersma and J. J. F. Scholten, *J. Catal.*, 1995, **152**, 130–136.
- 44 B. Xiang, C. Yu, H. Xu and W. Li, *Catal. Lett.*, 2008, **125**, 90–96.
- 45 S. Chen, Z. Qin, X. Xu and J. Wang, *Appl. Catal.*, A, 2006, **302**, 185–192.
- 46 A. Baiker, P. Dollenmeir, M. Glinski and A. Reller, *Appl. Catal.*, 1987, **35**, 351–364.
- 47 A. Gervasini, P. Carniti, J. Keranen, L. Niinisto and A. Auroux, *Catal. Today*, 2004, **96**, 187–194.
- 48 M. L. Ferreira and M. Volpe, *J. Mol. Catal. A: Chem.*, 2002, **184**, 349–360.
- 49 H. Zhao, S. Bennici, J. Shen and A. Auroux, *Appl. Catal.*, A, 2009, **356**, 121–128.
- 50 M. S. Marth, A. Wokaun, M. Pohl and H. L. Krauss, *J. Chem. Soc., Faraday Trans.*, 1991, **87**, 2635–2646.
- 51 F. Arena, F. Frusteri, G. Martra, S. Coluccia and A. Parmaliana, *J. Chem. Soc., Faraday Trans.*, 1997, **93**, 3849–3854.
- 52 H. Berndt, A. Martin, A. Bruckner, E. Schreier, D. Muller, H. Kosslick, G. U. Wolf and B. Lucke, *J. Catal.*, 2000, **191**, 384–400.
- 53 U. Scharf, M. S. Marth, A. Wokaun and A. Baiker, *J. Chem. Soc., Faraday Trans.*, 1991, **87**, 3299–3307.
- 54 S. D. Jackson and S. Rugmini, *J. Catal.*, 2007, **251**, 59–68.
- 55 Y. M. Liu, Y. Cao, N. Yi, W. L. Feng, W. L. Dai, S. R. Yan, H. Y. He and K. N. Fan, *J. Catal.*, 2004, **224**, 417–428.
- 56 A. Khodakov, J. Yang, S. Su, E. Iglesia and A. T. Bell, *J. Catal.*, 1998, **177**, 343–351.
- 57 M. A. Centeno, P. Malet, I. Carrizosa and J. A. Odriozola, *J. Phys. Chem. B*, 2000, **104**, 3310–3319.
- 58 S. Rajagopal, T. L. Grimm, D. J. Collins and R. Miranda, *J. Catal.*, 1992, **137**, 453–461.
- 59 M. M. Khader, *J. Mol. Catal. A: Chem.*, 1995, **104**, 87–94.
- 60 I. E. Wachs and B. M. Weckhuysen, *Appl. Catal.*, A, 1997, **157**, 67–90.
- 61 H. Miyata, K. Fujii and T. Ono, *J. Chem. Soc., Faraday Trans. 1*, 1988, **84**, 3121–3128.
- 62 N. Dhachapally, V. N. Kalevaru, A. Bruckner and A. Martin, *Appl. Catal.*, A, 2012, **443–444**, 111–118.
- 63 N. Dhachapally, V. N. Kalevaru, J. Radnik and A. Martin, *Chem. Commun.*, 2011, **47**, 8394–8396.
- 64 O. S. Owen and H. H. Kung, *J. Mol. Catal.*, 1993, **79**, 265–284.
- 65 M. C. Kung and H. H. Kung, *J. Catal.*, 1992, **134**, 668–677.
- 66 N. Dhachapally, V. N. Kalevaru and A. Martin, *Catal. Sci. Technol.*, 2014, **4**, 3306–3316.
- 67 J. Bilde, C. Janke, C. Lorentz, P. Delichere, I. Popescu, I. C. Marcu, S. Loridant, A. Bruckner and J. M. M. Millet, *J. Phys. Chem. C*, 2013, **117**, 22926–22938.
- 68 M. Niwa, H. Ando and H. Murakami, *J. Catal.*, 1977, **49**, 92–96.
- 69 J. Otamiri and A. Andersson, *Catal. Today*, 1988, **3**, 211–222.
- 70 P. Mars and D. W. van Krevelen, *Chem. Eng. Sci.*, 1954, **3**, 41–59.
- 71 P. Cavalli, F. Cavani, F. Manenti and F. Trifiro, *Ind. Eng. Chem. Res.*, 1987, **26**, 639–647.
- 72 G. Centi, F. Marchi and S. Perathoner, *Appl. Catal.*, A, 1997, **149**, 225–244.